# Compact grating couplers on silicon-on-insulator with reduced backreflection

Yanlu Li,[1,2,*] Diedrik Vermeulen,[1,2,3] Yannick De Koninck,[1,2] Gunay Yurtsever,[1,2] Günther Roelkens,[1,2] and Roel Baets[1,2]

[1]*Photonics Research Group, INTEC-department, Ghent University-IMEC, Sint-Pietersnieuwstraat 41, Ghent 9000, Belgium*

[2]*Center for Nano- and Biophotonics (NB-Photonics), Ghent University, Sint-Pietersnieuwstraat 41, Ghent 9000, Belgium*

[3]*Present address: Acacia Communications, Inc., 3 Clock Tower Place, Suite 210, Maynard, Massachusetts 01754, USA*

*Corresponding author: Yanlu.Li@intec.ugent.be*

The backreflection in commonly used grating couplers on silicon-on-insulator (SOI) is not negligible for many applications. This reflection is dramatically reduced in our improved compact grating coupler design, which directs the reflection away from the input waveguide. Realized devices on SOI show that the reflection can be reduced down to −50 dB without an apparent transmission penalty. © 2012 Optical Society of America

*OCIS codes:* 050.0050, 130.0130.

Surface grating coupler (GC) structures are extensively used in photonic integrated circuits (PICs) to couple light into and out of PICs. This coupling method does not require polished waveguide facets on the edge of a photonic chip, and can thus be used in wafer-scale testing of PICs. Improvements on the coupling efficiency and bandwidth of GC structures (to free space or to a single-mode fiber) have been thoroughly studied in recent publications [1–3]. Apart from that, the on-chip backreflection of GC structures is also often discussed, because it can deteriorate the behavior of some integrated components, e.g., an integrated laser. Two types of reflections may be introduced in a GC: the second-order Bragg reflection of the grating and the Fresnel reflection due to the mode mismatch between the grating region and the input waveguide. The zenith of the fiber $\phi$ (the angle between the normal of the PIC surface and the direction of the fiber) is often set as 10° or more to make sure that the second-order reflection is suppressed in the wavelength range of interest. However, the Fresnel reflection can still be reflected back to the waveguide. A suppression in the backreflection was reported by improving the mode matching between the grating region and input waveguide [4,5]. It was also reported that an apodized GC can be used to dramatically reduce the backreflection [6,7]. In this Letter, we experimentally demonstrate another method that can be used to strongly suppress the backreflection [8]. The devices are designed for the silicon-on-insulator (SOI) platform, but the concept can be extended to other photonic platforms.

The design is similar to the compact focusing grating couplers (FGCs) (without taper) reported by Van Laere *et al.* [9]. The trench shapes in these FGCs can be expressed in a polar coordinate system

$$r(q,\alpha) = \frac{q\lambda_0}{n_g - n_c \sin\phi \cos\alpha}, \qquad (1)$$

where $r(q,\alpha)$ represents the trench radius of the grating, $\alpha$ is the corresponding azimuth, $q \in N$ is the index of each line, $\lambda_0$ is the central wavelength of light in vacuum, $\phi$ is the zenith of the coupling direction in free space, and $n_g$ and $n_c$ are the effective indices of the grating region and the top cladding material, respectively. In this formula, it is assumed that the effective index value of the slab region $n_s$ is the same as $n_g$, which is, however, not exact. Considering this effective index difference, a more general equation is used in our design:

$$r(q,\alpha) = \frac{(q - q_0) \cdot \lambda_0}{n_g - n_c \sin\phi \cos\alpha} + p(q_0,\alpha), \qquad (2)$$

where

$$p(q_0,\alpha) = \frac{\kappa q_0 \lambda_0}{n_s - n_c \sin\phi \cos\alpha}, \qquad (3)$$

$q_0 \in N$ is the index of the first line in the grating, and $\kappa$ is a factor to determine the distance $L$ between the first line and the entrance waveguide. In this Letter, $\kappa$ is chosen as $(n_s - n_c \sin\phi)/(n_g - n_c \sin\phi)$ so that $r(q_0,0)$ is the same as that from the conventional design. A similar correction was also reported in [10].

These curves form an array of ellipses with their first focus points $f_{1,q}$ at the same position. According to Eq. (2), if the end of the entrance waveguide is located on $f_{1,q}$, light coming from this waveguide can be coupled out of the chip to the predesigned direction in free space. In previously used FGCs [9] (standard FGCs), the entrance waveguide points to the grating region with $\alpha = 0°$ [seen in Fig. 1(a)]. Actually, light can be coupled to almost the same predesigned direction if the entrance waveguide is rotated around $f_{1,q}$ and another part of the grating is used (the actual coupling direction might be slightly different due to the second-order reflection). In this case, the backreflection that is refocused on a location near the second focus points of the ellipses $f_{2,q}$ will not be coupled back in the entrance waveguide [seen in Fig. 1(b)]. As a result, the reflection back into the entrance waveguide is suppressed. The reduced reflection in this design has been demonstrated by means of simulation [11,12], and the results show that the backreflection of FGCs with $\alpha = 45°$ or $90°$ are suppressed compared to standard FGCs. Besides, to avoid the
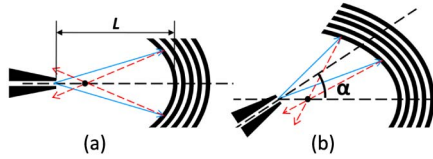
Fig. 1. (Color online) Schematic of tilted FGCs (exaggerated) on SOI with different azimuths: (a) $\alpha = 0$ and (b) $\alpha \neq 0$. The black region is etched 70 nm into a 220 nm silicon layer, while the rest is unetched. The light diffracting from the waveguide and the Fresnel reflections is indicated with the solid and dashed blue and red lines, respectively.



Fig. 3. (Color online) Transmission spectra of the tilted FGCs with different azimuths.

influence to the adjacent devices, the backreflection can be collected to another waveguide and then sent to a high-loss region. This design slightly breaks the symmetry of the output mode, but its influence on the grating-to-fiber coupling is not much when $\phi = 10°$. The new design (titled FGC) also has a very compact size compared to the commonly used one-dimensional (1D) GC.

Tilted FGCs with different $\alpha$ have been fabricated using deep UV (193 nm) lithography through the ePIXfab multiproject wafer service [13], and they are designed to couple 1550 nm light with $\phi = 10°$. The width of the entrance waveguide aperture (0.9 µm) was chosen to be neither too small to introduce extra reflection nor too large to collect the redirected Fresnel reflection from the grating. The distance $L$ determines the size of the output mode in the GC and thus influences the maximal grating-to-single-mode-fiber coupling efficiency $\eta$. In order to know the optimal value of $L$, a number of FGCs ($\alpha = 0°$) with different first grating indices $q_0$ were fabricated and measured. The $\eta$ values of different FGCs and the corresponding central wavelengths $\lambda_0$ are plotted in Fig. 2. It is found that the best $q_0$ is 26, which means $L = 16$ µm. All the following designs use this $q_0$ value. The variation of the $\lambda_0$ is within 5 nm, and it might be caused by the alignment variations of fibers.

Designs with two identical tilted FGCs connected by a shallowly etched waveguide were measured to retrieve $\eta$ for different $\alpha$. These transmission spectra are plotted in Fig. 3. The $\eta$ and $\lambda_0$ values are plotted in Fig. 4. The solid horizontal line in Fig. 4 stands for the $\eta$ of a standard FGC (−4.6 dB). It can be found that the $\lambda_0$ values are lower than 1550 nm. Two main reasons are responsible for this shift: (1) $n_g$ and $\phi$ are wrongly estimated in the design, and the real central wavelength will thus become $\lambda' = \lambda_0 (n'_g - n_c \sin \phi' \cos \alpha)/(n_g - n_c \sin \phi \cos \alpha)$, where $n'_g$ and $\phi'$ stand for the real values of $n_g$ and $\phi$, respectively. It is seen that $\lambda'$ is a function of $\alpha$, which is also shown in
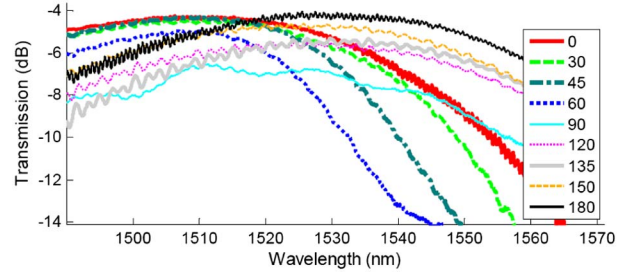
the measurement results. (2) A dip caused by the second-order reflection exists in the transmission spectra of the tilted FGCs with $\alpha$ close to 90°, and this reflection dip causes both a suppression of $\eta$ and a shift of $\lambda_0$. Note that the central wavelength of the second-order reflection has a blueshift as $\alpha$ increases. For $\alpha \geq 150°$ or $\leq 60°$, the $\lambda_0$ of the second-order reflection stays far away from the transmission band and thus has less influence. The second-order reflection also causes a bandwidth increase in the tilted FGCs with $\alpha$ close to 90°.

It is hard to estimate the reflections using the fringes in the transmission spectrum, because the reflections on the output fiber end facets are also mixed in the spectrum. In order to measure the reflection values of our tilted FGCs, we use another set of samples. In those samples, all the input FGCs use the same design with $\alpha = 0°$, while the output tilted FGCs have a scan of the azimuth from 0° to 180°. The frequency average reflections are measured by a simplified optical frequency domain reflectometry setup [14]. First we align the input fiber with the help of an output fiber. After alignment, the output fiber is moved away so that the influence caused by the reflection of the output fiber facet is removed. With the help of a circulator, the reflected light signal including reflections from the input fiber facet and reflections from the reflective components in the waveguide is retrieved. A wavelength sweep from 1490 to 1570 nm with a 20 pm resolution was done to obtain the reflection spectrum. The postprocessing on the reflection spectrum is done in a computer, and a spatial distribution of the reflection is calculated from the autocorrelation $R(z)$ of the reflection spectrum. Three steps are done before calculating $R(z)$: (1) interpolating the reflection spectra from the wavelength domain to the frequency domain, (2) multiplying a Gaussian window to the spectrum in the frequency domain, so as to suppress numerical leakages [15], and (3) zero padding, in order to get a denser frequency mesh
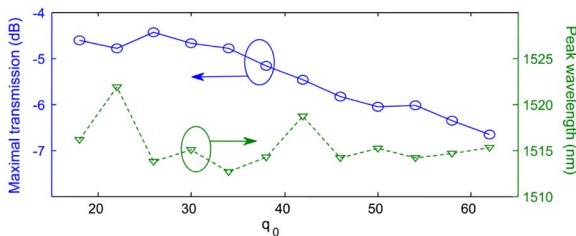


Fig. 2. (Color online) Maximal coupling efficiency between a single-mode fiber and FGCs with different $q_0$ values and corresponding central wavelengths. The width of the waveguide aperture is 0.9 µm.
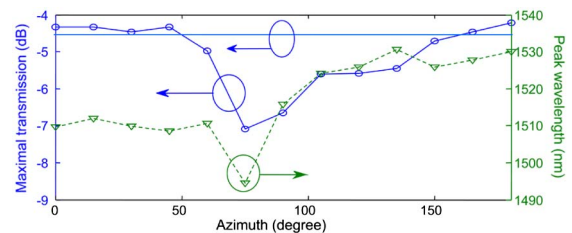


Fig. 4. (Color online) Maximal transmission efficiencies of the tilted FGCs and the corresponding wavelengths. The horizontal line stands for the $\eta$ of a standard FGC.
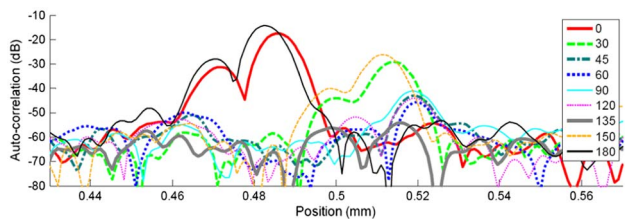
Fig. 5.    (Color online) Peaks in the autocorrelation $R(z)$ caused by the reflection from the output tilted GCs with different azimuths. The autocorrelations are plotted in a logarithmic scale $(20 \times \log(R(z)))$.
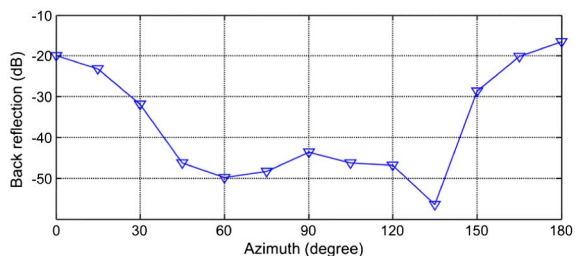


Fig. 6.    (Color online) Maximal frequency average reflections of the tilted FGCs for different azimuths.

in the autocorrelation function, which is good for estimating the 3 dB bandwidth of peaks. After these steps, a power spectral density $P(f)$ for an array of frequencies $f$ was obtained. $R(z)$ was then derived by calculating the inverse Fourier transform of $P(f)$.

The distances between the input and output tilted FGCs are around 500 μm, but not exactly the same. The reflection autocorrelations $R(z)$ for different azimuths with $z$ near 500 μm are plotted in Fig. 5. Two maximal values can be found for each sample, which means that two different reflections are correlated with the reflection at the output tilted FGC. They are the reflections from the input fiber facet and from the input GC, respectively, and the former one corresponds to a larger $z$. The reflectance values of the tilted FGCs are obtained by calculating the integral over the 3 dB bandwidth around $\lambda_0$. The frequency average reflections for different $\alpha$ are plotted in Fig. 6. Assuming that a 4% reflection occurs at the input fiber facet, the frequency average reflection for an FGC with $\alpha = 0°$ is around −20 dB. GCs with $\alpha$ between 45° and 135° have the frequency average back-reflection suppressed to less than −40 dB. The best reflection suppression is for $\alpha = 135°$, which is around −55 dB. The optimal $\alpha$ is not 90°, and that is because the central wavelength value of the second-order reflection is near the transmission peak in this case. This is also shown in the simulation results [11,12].

For tilted FGCs with the azimuth $\alpha$ in the range between 45° and 60°, the frequency average reflection is highly suppressed (up to −50 dB) with no apparent transmission penalty. In this design, the Fresnel reflection is directed away from the entrance waveguide rather than being suppressed. This design can work together with the other GC structures that have reduced Fresnel reflection (e.g., apodized gratings), so as to further suppress the on-chip back reflection of the GC strucutures.

**References**

1. D. Taillaert, F. Van Laere, M. Ayre, W. Bogaerts, D. Van Thourhout, P. Bienstman, and R. Baets, Jpn. J. Appl. Phys. **45**, 6071 (2006).
2. D. Vermeulen, S. Selvaraja, P. Verheyen, G. Lepage, W. Bogaerts, P. Absil, D. V. Thourhout, and G. Roelkens, Opt. Express **18**, 18278 (2010).
3. A. Mekis, S. Gloeckner, G. Masini, A. Narasimha, T. Pinguet, S. Sahni, and P. De Dobbelaere, IEEE J. Sel. Topics. Quantum Electron. **17**, 597 (2011).
4. C. Alonso-Ramos, A. Ortega-Monüx, I. Molina-Fernández, P. Cheben, L. Zavargo-Peche, and R. Halir, Opt. Express **18**, 15189 (2010).
5. N. Na, H. Frish, I.-W. Hsieh, O. Harel, R. George, A. Barkai, and H. Rong, Opt. Lett. **36**, 2101 (2011).
6. M. Antelius, K. B. Gylfason, and H. Sohlström, Opt. Express **19**, 3592 (2011).
7. R. Halir, P. Cheben, S. Janz, D.-X. Xu, Í. Molina-Fernández, and J. G. Wangüemert-Pérez, Opt. Lett. **34**, 1408 (2009).
8. Y. Li, D. Vermeulen, Y. De Koninck, G. Yurtsever, G. Roelkens, and R. Baets, in *Proceedings of Optical Fiber Communication Conference (OFC)* (Optical Society of America, 2012), p. JTh2A.8.
9. F. Van Laere, T. Claes, J. Schrauwen, S. Scheerlinck, W. Bogaerts, D. Taillaert, L. O'Faolain, D. Van Thourhout, and R. Baets, IEEE Photon. Technol. Lett. **19**, 1919 (2007).
10. R. Waldhäusl, B. Schnabel, P. Dannberg, E.-B. Kley, A. Bräuer, and W. Karthe, Appl. Opt. **36**, 9383 (1997).
11. D. Vermeulen, Y. De Koninck, Y. Li, E. Lambert, W. Bogaerts, R. Baets, and G. Roelkens, in *8th International Conference in Group IV Photonics* (IEEE, 2011), p. 74 (P1.6).
12. D. Vermeulen, Y. De Koninck, Y. Li, W. Bogaerts, R. Baets, and G. Roelkens, Opt. Express **20**, 22278 (2012).
13. http://www.epixfab.eu.
14. F. Morichetti, A. Canciamilla, C. Ferrari, M. Torregiani, A. Melloni, and M. Martinelli, Phys. Rev. Lett. **104**, 033902 (2010).
15. F. J. Harris, Proc. IEEE **66**, 51 (1978).